JOURNAL OF OPTOELECTRONICS AND ADVANCED MATERIALS, Vol. 11, No. 6, June 2009, p. 782 - 789

Manipulation of Cs atoms with laser fields scattered by metallic thin films

S.-B. BALMUS*, D. D. SANDU[a], G.-O. AVADANEI[a], G.-N. PASCARIU[a]
Science Department, "Al. I. Cuza" University of IASI, Romania
[a]Faculty of Physics, "Al. I. Cuza" University of IASI, Romania

Manipulation of atoms with laser fields is a very important physical process in controlling atom flux for direct "nano" writing on surfaces, building photosensitive nanophotocathode arrays on semiconductors and guiding atoms through surface-plasmon and resonant-ring structures.

(Received May 18, 2009; accepted June 15, 2009)

Keywords: Atom manipulation, Scattered laser fields, Metallic nano thin film, Cs two-level atom model

1. Introduction

In this paper we present the most important relations regarding the interaction of electromagnetic laser fields with the Cs "two-level atom" based on Schrödinger equation. The laser field scattered by a periodic metallic nano thin film acts on Cs atom trajectories in the near field region. Also, some results concerning the possibility and the conditions to use these fields for Cs atoms manipulation are discussed.

2. The two-level model of cs atom

For characterizing the interaction between a Cs atom and an electromagnetic laser field with a frequency ω closed to Cs s-p transition, the two-level model of the Cs atom, using the electronic basis functions $|s,0\rangle, |p,-1\rangle, |p,0\rangle, |p,1\rangle$, is presented in Fig. 1. [1].

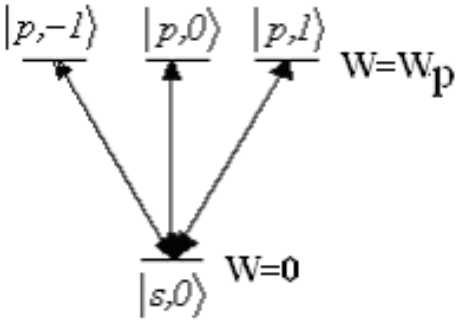

Fig. 1. The two-level Cs atom model

The Schrödinger equation for electrons has the form [2,3]:

$$i\hbar|\dot{\Psi}\rangle = \left(H_{el} - \vec{d}\cdot\hat{e}E_0\cos\omega t\right)|\Psi\rangle \quad (1)$$

where H_{el} is the electronic Hamiltonian, $\vec{d}$ is the dipole moment of the atom, $\hat{e}$ is the unit vector of the electric field, E_0 is the electric field amplitude and ω the pulsation of the electromagnetic laser field.

The wave function $|\Psi\rangle$ and its derivate $|\dot{\Psi}\rangle$ have the expressions:

$$\begin{aligned}|\Psi\rangle &= c_0|s,0\rangle + c_1|p,-1\rangle + c_2|p,0\rangle + c_3|p,1\rangle \\ |\dot{\Psi}\rangle &= \dot{c}_0|s,0\rangle + \dot{c}_1|p,-1\rangle + \dot{c}_2|p,0\rangle + \dot{c}_3|p,1\rangle\end{aligned} \quad (2)$$

where c_0, c_1, c_2, c_3 are the electronic basis function's coefficients and $\dot{c}_0, \dot{c}_1, \dot{c}_2, \dot{c}_3$ represent their derivates.

Equation (1) can be expressed using the electronic basis functions as follows [3, 4]

$$i\hbar\begin{bmatrix}\dot{c}_0\\ \dot{c}_1\\ \dot{c}_2\\ \dot{c}_3\end{bmatrix} = [A]\begin{bmatrix}c_0\\ c_1\\ c_2\\ c_3\end{bmatrix} \quad (3)$$

or

$$i\hbar\begin{bmatrix}\dot{c}_0\\ \dot{c}_1\\ \dot{c}_2\\ \dot{c}_3\end{bmatrix} = \begin{bmatrix}0 & M_{01}\cos\omega t & M_{02}\cos\omega t & M_{03}\cos\omega t\\ M_{10}\cos\omega t & E_p & 0 & 0\\ M_{20}\cos\omega t & 0 & E_p & 0\\ M_{30}\cos\omega t & 0 & 0 & E_p\end{bmatrix}\begin{bmatrix}c_0\\ c_1\\ c_2\\ c_3\end{bmatrix} \quad (4)$$

where the following notations are used:

$$
\begin{aligned}
M_{01} &= -\langle s,0|\vec{d}\cdot\hat{e}|p,-1\rangle E_0 \\
M_{02} &= -\langle s,0|\vec{d}\cdot\hat{e}|p,0\rangle E_0 \\
M_{03} &= -\langle s,0|\vec{d}\cdot\hat{e}|p,1\rangle E_0 \\
M_{10} &= -\langle p,-1|\vec{d}\cdot\hat{e}|s,0\rangle E_0 \\
M_{20} &= -\langle p,0|\vec{d}\cdot\hat{e}|s,0\rangle E_0 \\
M_{30} &= -\langle p,1|\vec{d}\cdot\hat{e}|s,0\rangle E_0
\end{aligned}
\tag{5}
$$

Using the transformations of variables:

$$
\begin{aligned}
d_0 &= c_0 & \dot{d}_0 &= \dot{c}_0 \\
d_1 &= e^{i\omega t}c_1 & \dot{d}_1 &= i\omega e^{i\omega t}c_1 + e^{i\omega t}\dot{c}_1 \\
d_2 &= e^{i\omega t}c_2 & \dot{d}_2 &= i\omega e^{i\omega t}c_2 + e^{i\omega t}\dot{c}_2 \\
d_3 &= e^{i\omega t}c_3 & \dot{d}_3 &= i\omega e^{i\omega t}c_3 + e^{i\omega t}\dot{c}_3
\end{aligned}
\tag{6}
$$

Schrödinger equation becomes

$$
\begin{aligned}
&i\hbar\dot{d}_0 = i\hbar\dot{c}_0 = M_{01}\cos\omega t c_1 + M_{02}\cos\omega t c_2 + \\
&+ M_{03}\cos\omega t c_3 = M_{01}\cos\omega t e^{-i\omega t}d_1 + \\
&+ M_{02}\cos\omega t e^{-i\omega t}d_2 + M_{03}\cos\omega t e^{-i\omega t}d_3 \\
&i\hbar\dot{d}_1 = -\hbar\omega d_1 + e^{i\omega t}M_{10}\cos\omega t c_0 + e^{i\omega t}E_p c_1 \\
&= (E_p - \hbar\omega)d_1 + M_{10}\cos\omega t e^{i\omega t}d_0 \\
&i\hbar\dot{d}_2 = -\hbar\omega d_2 + e^{i\omega t}M_{20}\cos\omega t c_0 + e^{i\omega t}E_p c_2 \\
&= (E_p - \hbar\omega)d_2 + M_{20}\cos\omega t e^{i\omega t}d_0 \\
&i\hbar\dot{d}_3 = -\hbar\omega d_3 + e^{i\omega t}M_{30}\cos\omega t c_0 + e^{i\omega t}E_p c_3 \\
&= (E_p - \hbar\omega)d_3 + M_{30}c\ \ os\omega t e^{i\omega t}d_0
\end{aligned}
\tag{7}
$$

In the "rotating wave approximation" RWA [3] we can write

$$
\begin{aligned}
e^{-i\omega t}\cos\omega t &= \frac{1}{2}\left(1 + e^{-2i\omega t}\right) \approx \frac{1}{2} \\
e^{i\omega t}\cos\omega t &= \frac{1}{2}\left(1 + e^{2i\omega t}\right) \approx \frac{1}{2}
\end{aligned}
\tag{8}
$$

Schrödinger equation takes the form:

$$
i\hbar\begin{bmatrix}\dot{d}_0\\ \dot{d}_1\\ \dot{d}_2\\ \dot{d}_3\end{bmatrix} = \begin{bmatrix} 0 & \frac{1}{2}M_{01} & \frac{1}{2}M_{02} & \frac{1}{2}M_{03} \\ \frac{1}{2}M_{10} & -\Delta & 0 & 0 \\ \frac{1}{2}M_{20} & 0 & -\Delta & 0 \\ \frac{1}{2}M_{30} & 0 & 0 & -\Delta \end{bmatrix}\begin{bmatrix} d_0\\ d_1\\ d_2\\ d_3\end{bmatrix}
\tag{9}
$$

where $\Delta = (\hbar\omega - W_p) = \hbar\delta$ is the detuning between the laser frequency and the Cs atom s-p transition frequency.

For weak field and large detuning, we have $\dot{d}_1 \approx 0,\ \dot{d}_2 \approx 0, \dot{d}_3 \approx 0$ and Schrödinger equation is

$$
\begin{cases}
i\hbar\dot{d}_0 = \frac{1}{2}M_{01}d_1 + \frac{1}{2}M_{02}d_2 + \frac{1}{2}M_{03}d_3 \\
0 = \frac{1}{2}M_{10}d_0 - \Delta d_1 \rightarrow d_1 = \frac{M_{10}}{2\Delta}d_0 \\
0 = \frac{1}{2}M_{20}d_0 - \Delta d_2 \rightarrow d_2 = \frac{M_{20}}{2\Delta}d_0 \\
0 = \frac{1}{2}M_{30}d_0 - \Delta d_3 \rightarrow d_3 = \frac{M_{30}}{2\Delta}d_0
\end{cases}
\tag{10}
$$

Including the last three equations of the system (10) in the first one, we obtain the "one-level-atom" model [3], [4]

$$
i\hbar\dot{d}_0 = \frac{1}{4\Delta}\left(M_{01}M_{10} + M_{02}M_{20} + M_{03}M_{30}\right)d_0 \tag{11}
$$

or

$$
i\hbar\dot{d}_0 = U_{eff}\,d_0 \tag{12}
$$

where U_{eff} is the effective potential energy which characterizes the laser field and atom interaction:

$$
\begin{aligned}
U_{eff} &= \frac{E_0^2}{4\Delta}\left[\langle s,0|\vec{d}\cdot\hat{e}|p,-1\rangle\langle p,-1|\vec{d}\cdot\hat{e}|s,0\rangle + \right. \\
&\left. + \langle s,0|\vec{d}\cdot\hat{e}|p,0\rangle\langle p,0|\vec{d}\cdot\hat{e}|s,0\rangle + \langle s,0|\vec{d}\cdot\hat{e}|p,1\rangle\langle p,1|\vec{d}\cdot\hat{e}|s,0\rangle\right]
\end{aligned}
\tag{13}
$$

Next we will calculate the matrix elements $\langle s,0|\vec{d}\cdot\hat{e}|p,0,\pm1\rangle$. The scalar product $\vec{d}\cdot\hat{e}$ is:

$$
\vec{d}\cdot\hat{e} = \sum_{p,q}(-1)^p E_{-p}d_q \tag{14}
$$

The electronic wave functions, using spherical electronic basis function $Y_{l,q}(\theta,\phi)$, are [3]:

$$
\begin{aligned}
\langle r|s,0\rangle &= R_s(r)Y_{0,0}(\theta,\phi) \\
\langle r|p,-1\rangle &= R_p(r)Y_{0,0}(\theta,\phi) \\
\langle r|p,0\rangle &= R_p(r)Y_{0,0}(\theta,\phi) \\
\langle r|p,1\rangle &= R_p(r)Y_{0,0}(\theta,\phi)
\end{aligned}
\tag{15}
$$

Therefore

$$
\langle s,0|\vec{d}\cdot\hat{e}|p,0,\pm1\rangle = \sum_{p,q}(-1)^p E_{-p}\langle s,0|d_q|p,0,\pm1\rangle \tag{16}
$$

where

$$
d_q = -\sqrt{\frac{4\pi}{3}}rY_{1,q}(\theta,\phi) \tag{17}
$$

From equations (15), (16) and (17) we obtain

$$\begin{aligned}\langle s,0|d_q|p,m\rangle &= -\sqrt{\frac{4\pi}{3}}e\left[\int_0^\infty r^3 dr R_s^*(r)R_p(r)\right]\cdot \\ &\cdot\left[\int_0^\pi \sin\theta d\theta \int_0^{2\pi} d\phi Y_{00}^*(\theta,\phi)Y_{1,q}(\theta,\phi)Y_{1,m}(\theta,\phi)\right] = \\ &= -\sqrt{3}e\left[\int_0^\infty r^3 dr R_s^*(r)R_p(r)\right]\langle 11;00|00\rangle\cdot\langle 11;m,q|00\rangle\end{aligned} \tag{18}$$

Hence:

$$\begin{aligned}\langle s,0|\vec{d}\cdot\hat{e}|p,-1\rangle &= d_{sp}\sum_p (-1)^p E_{-p}\langle s,0|d_1|p,-1\rangle = \\ &= \frac{-d_{sp}}{\sqrt{3}}\sum_p (-1)^p E_{-p} = \frac{-d_{sp}}{\sqrt{3}} \\ \langle s,0|\vec{d}\cdot\hat{e}|p,0\rangle &= d_{sp}\sum_p (-1)^p E_{-p}\langle s,0|d_0|p,0\rangle = \\ &= \frac{d_{sp}}{\sqrt{3}}\sum_p (-1)^p E_{-p} = -\frac{d_{sp}}{\sqrt{3}} \\ \langle s,0|\vec{d}\cdot\hat{e}|p,1\rangle &= d_{sp}\sum_p (-1)^p E_{-p}\langle s,0|d_{-1}|p,1\rangle = \\ &= \frac{-d_{sp}}{\sqrt{3}}\sum_p (-1)^p E_{-p} = \frac{-d_{sp}}{\sqrt{3}}\end{aligned} \tag{19}$$

and the effective energy of interaction becomes

$$\begin{aligned}U_{eff} &= \frac{E_0^2}{4\Delta}\left[\left|\langle s,0|\vec{d}\cdot\vec{\varepsilon}|p,-1\rangle\right|^2 + \left|\langle s,0|\vec{d}\cdot\vec{\varepsilon}|p,0\rangle\right|^2 + \right. \\ &\left. + \left|\langle s,0|\vec{d}\cdot\vec{\varepsilon}|p,1\rangle\right|^2\right] = \frac{E_0^2 d_{sp}^2}{4\Delta} = \frac{E_0^2 d_{sp}^2}{4\hbar\delta}\end{aligned} \tag{20}$$

The motion equations of Cs atoms is governed by the Hamiltonian [5]

$$H = \frac{\vec{p}^2}{2m} + U(\vec{r}) = \frac{\vec{p}^2}{2m} + \frac{E_0^2 d_{sp}^2}{4\hbar\delta}, \qquad U(\vec{r}) = \frac{E_0^2 d_{sp}^2}{4\hbar\delta} \tag{21}$$

where

$$\begin{cases} \dot{x} = \dfrac{p_x}{m} \\ \dot{y} = \dfrac{p_y}{m} \\ \dot{z} = \dfrac{p_z}{m} \\ \dot{p}_x = -\partial U/\partial x \\ \dot{p}_y = -\partial U/\partial y \\ \dot{p}_z = -\partial U/\partial z \end{cases} \quad or \quad \begin{cases} \dot{x} = v_x \\ \dot{y} = v_y \\ \dot{z} = v_z \\ \dot{v}_x = -\dfrac{\partial U/\partial x}{m} \\ \dot{v}_y = -\dfrac{\partial U/\partial y}{m} \\ \dot{v}_z = -\dfrac{\partial U/\partial z}{m} \end{cases} \tag{22}$$

In the case of an electromagnetic laser field scattered by a particular diffraction structure it is convenient to have the potential energy as a function of the ratio between the incident and the scattered electric field. Using the intensity of the laser field we can write for the expression of the potential energy

$$U(\vec{r}) = \frac{d_{sp}^2}{4\hbar\delta}\frac{2I_0}{\varepsilon_0 c}\frac{E^2}{E_0^2} = \frac{d_{sp}^2}{2\hbar\delta}\frac{I_0}{\varepsilon_0 c}\frac{E(\vec{r})^2}{E_0^2} \tag{23}$$

where $I_0\left(W/m^2\right)$ is the intensity of the incident laser field, E_0 is the magnitude of the incident electric field on the scattering micro or nanostructure; $E(\vec{r})$ is the magnitude of the total electric field; $\varepsilon_0 = 8.854\times10^{-12}\ F/m$ is the permittivity of free space; $\hbar = 1.054\times10^{-34}\ J\cdot s$ is Planck's constant and c is the light speed in free space.

For Cs: $m = 133\ a.m.u.* = 2.2\times10^{-25}\ Kg$

and $d_{sp}^2 = 12.2\cdot a_0^2\cdot q^2 = 8.74\times10^{-58}\left(C\cdot m\right)^2$

where:

$a_0 = 0.529\times10^{-10}\ m$ is the Bohr-Radius

$q = 1.6\times10^{-19}\ C$ is the electronic charge.

* *a.m.u* – atomic mass unity $1\ a.m.u = 1.660\times10^{-27}\ Kg$

3. Movement of Cs atoms in the near field of a metallic thin film with periodical rectangular holes. Simulation procedures

The scattering array, presented in figure 2, consists of a metallic nano thin film which is characterized by a *300nm* depth and square *300nm* holes situated at *505nm* one from each other. The film is considered periodical and infinite along Ox and Oy axis and its inferior face is characterized by *z=0*. The main purpose of the simulations presented below is to verify if it is possible to obtain a periodical nano photocathode network using the near field scattered by the thin film for guiding the Cs atoms and deposing them in a periodical nano array (rows or groups of atoms).

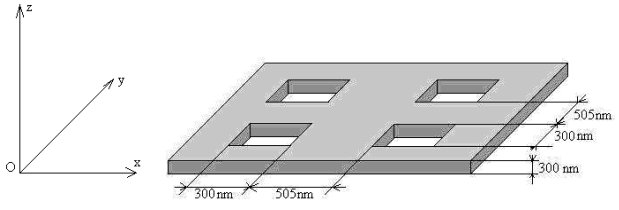

Fig. 2. The metallic film and its dimensions

The metallic film is excited from below (*z<0*) with electromagnetic laser plane waves with a wavelength of *854nm*

3.1. Scattered field's structure

Using the momentum method [6,8], the relative electromagnetic field structure was calculated above the metallic film (z>0) and it is presented in this section. The relative field is defined as the ratio between the total (incident and scattered) field and the incident field. One example of the electric field structure calculated above the metallic nano thin film is presented in Fig. 3.

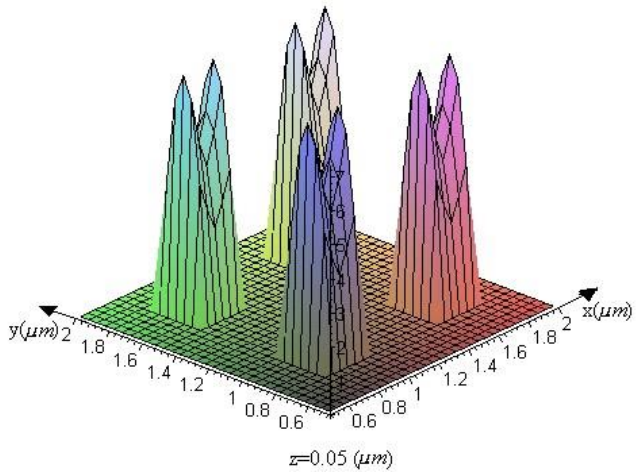

Fig. 3. Relative electric field in cross section at z = 0.05 μm

Because of the nano metallic thin film periodicity, bellow is presented the relative field structures (Fig. 5.6.7.8) corresponding to one period; this is a 805nm square centered on *(980,980,0) nm* as shown in Fig. 4. [10-12]

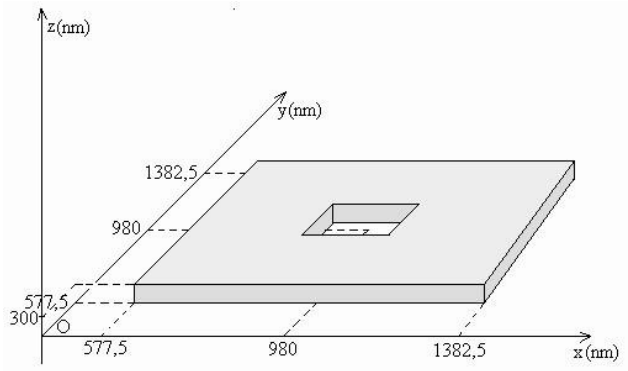

Fig. 4. One period of the metallic thin film

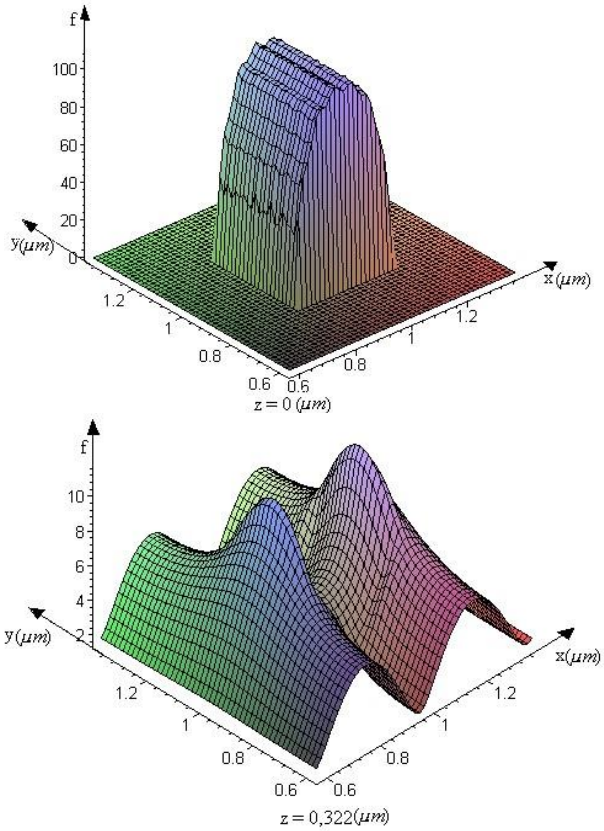

Fig. 5. Relative electric field in cross section at z = 0 μm and z=0.322 μm

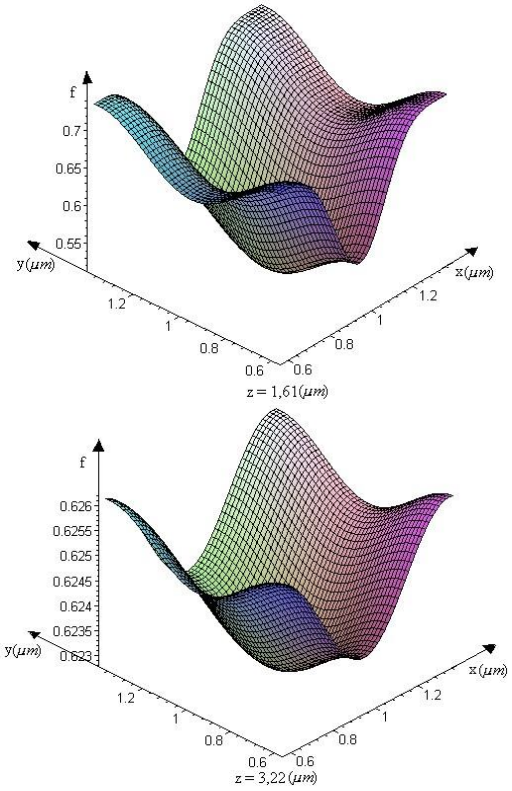

Fig. 6. Relative electric field in cross section at z = 1.61 μm and z=3.22 μm

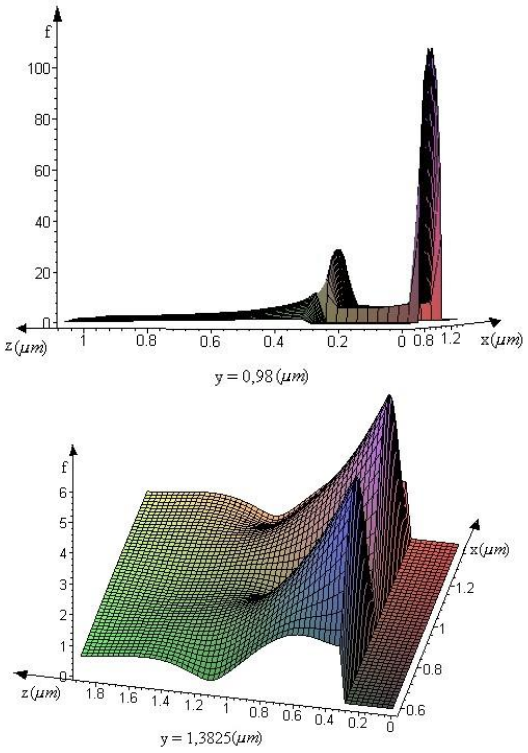

Fig. 7. Relative electric field in cross section at y = 0.98 μm (middle of the hole) and y = 1.3825 μm (between the holes)

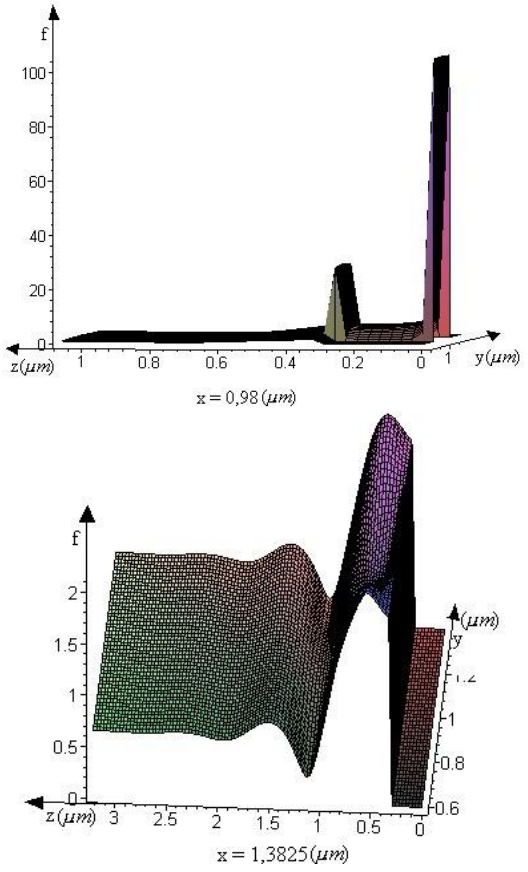

Fig. 8. Relative electric field in cross section at x = 0.98 μm (middle of the hole) and y = 1.3825 μm (between the holes).

3.2. Manipulation of Cs atoms in the described fields trajectories

The potential energy (23) is equivalent with

$$U(\vec{r}) = \frac{d_{sp}^2}{2\hbar\delta}\frac{I_0}{\varepsilon_0 c}\left(\frac{E(\vec{r})}{E_0}\right)^2 = B\frac{I_0}{\delta}\left(\frac{E(\vec{r})}{E_0}\right)^2 \qquad (24)$$

where

$$B = \frac{d_{sp}^2}{2\hbar\varepsilon_0 c} \approx 0.156\times 10^{-20} \quad (S.I.\ unities)$$

$$B = \frac{d_{sp}^2}{2\hbar\varepsilon_0 c} \approx 0.0941\times 10^{13} \quad (nm.\ \mu s.\ a.m.u.\ unities)$$

So, the potential interaction energy becomes

$$U(\vec{r}) = 941\frac{I_0\left(W/m^2\right)}{\delta(GHz)}\left(\frac{E(\vec{r})}{E_0}\right)^2 \qquad (25)$$

Depending on the detuning between the laser frequency and Cs s-p transition frequency, to the red (negative) or to the blue (positive), the force which acts between the Cs atoms and the electromagnetic field is attractive or repulsive.

The main purpose of the calculus of the trajectories is to verify if the metallic film and the scattered field could be used for guiding the atoms through the holes and deposing them on a semiconductor substrate or to depose the atoms directly on a semiconductor substrate on the top of the metallic film on one side and the other of the apertures. So, a nano periodical atoms structure (network) with photosensitive proprieties could be obtain.

For the calculus of the trajectories it is used a Finite Element method [9] with the next steps:

- space division in cubic elements in which the field could be approximate as constant along Ox, Oy and Oz axis. So, the atoms movement can be considered as a Newtonian uniform accelerate movement and because of relative small velocities the relativistic effects are ignored.
- the gravitational and interaction between the Cs atoms forces are ignored; so, only the electromagnetic fields effect can be observed.
- a small time step selection (choice) in order to not exceed the finite element limit in one integration (the spatial step is ten times smaller then the cube size).
- integration of the scalar movement equations.

As a source of Cs atoms it is used a MOT (Magneto Optical Trap) [7] with a temperature $T = 50\mu K - 100\mu K$ situated at *z=2012.5 nm* above the film. In the trajectories calculus it is used a $\delta = 10GHz$ detuning and an $I_0 = 5\times 10^5 W/m^2$ incident electromagnetic field intensity. The initial position of Cs atoms is characterized by *z=2012.5nm* and randomly *x* and *y* between *577.5 nm*

and *1382.5 nm;* the initial velocity of Cs atoms on *z* is $v_{0z} = -1\times10^3 \div -5\times10^4\ nm/\mu s$.

The initial velocity on Oz axis is considered negative because it is orientated in opposite sense with the *Oz* direction.

3.2.1. Attractive force

Taking into account 10^5 atoms it was calculated the number of atoms which arrived in the hole, as a function of the initial velocity on *Oz* direction. Randomly positions on Ox and Oy were generated and it was obtained a number of *14003* atoms which were initially in direction of the hole ($z_0 = 2012.5nm;\ x_0$ *and* y_0 *between* $830nm and 1130nm$). The number of atoms which finally arrived in the hole ($z \le 301.875nm;$ *x and y between* $830nm and 1130nm$), as a function of the initial velocity on *Oz*, is presented in Fig.9.

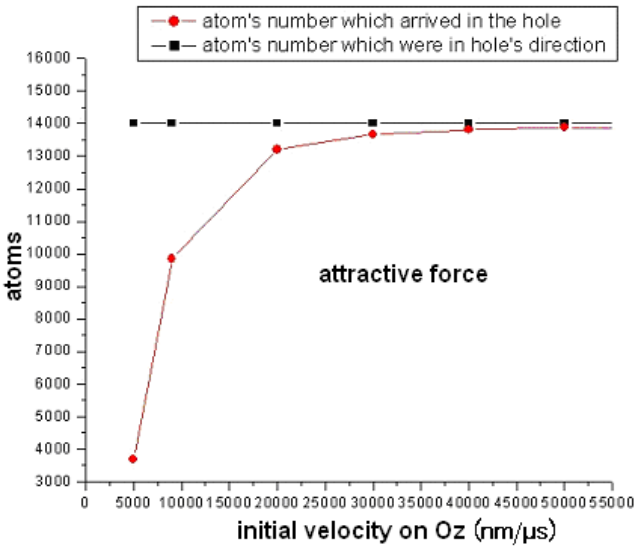

Fig. 9. The number of atoms which arrived in the hole

It can be seen from Fig. 9. that the field effect is important for initial velocity on *Oz* smaller than $15\times10^3\ nm/\mu s$. For initial velocities greater than $20\times10^3\ nm/\mu s$ the effect of the field is negligible. The time of interaction between the field and the atoms is too small and the initial kinetic energy of Cs atoms is greater then the potential energy of interaction between the field and the atoms. Also, it can be seen that the number of atoms which arrive in the hole decreases when the initial velocity on *Oz* decreases. The time of interaction between the field and that Cs atoms increases and so the effect of the field is greater. The fact that the atoms did not arrive in the hole is due to the field configuration. As it can be seen in Fig. 6, the electric field is greater on a side and on the other of the hole and in the "attractive force" case the atoms will migrate there where the field is greater.

To see exactly what is happening with the Cs atoms in the described attractive field, trajectories were calculated and represented in Fig. 10 and Fig.11. [10-12]

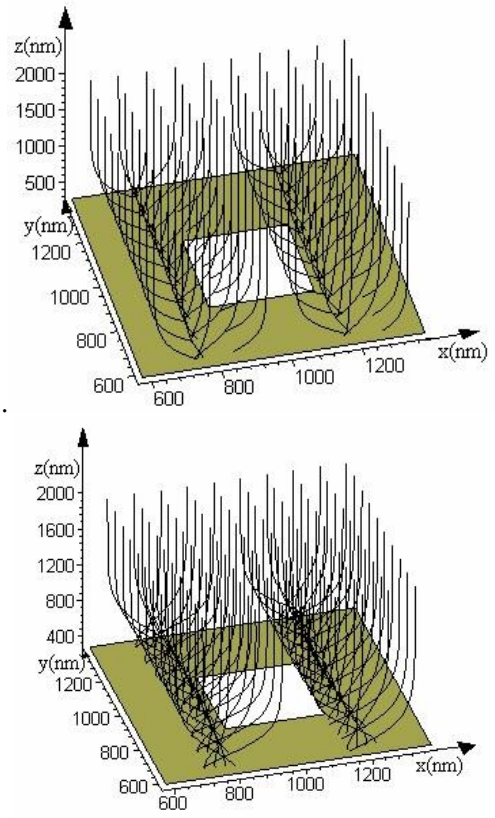

Fig. 10. 100 trajectories for v_{0z} = -5000 nm/μs and v_{0z} = -3000 nm/μs

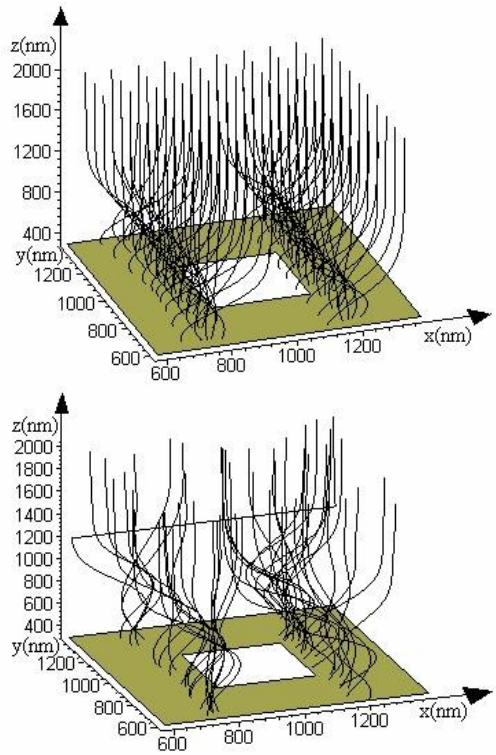

Fig. 11. 100 trajectories for v_{0z} = -2000 nm/μs and 50 trajectories for v_{0z} = -1000 nm/μs

3.2.2 Repulsive force

Taking into account 10^5 atoms it was calculated the number of atoms which arrived in the hole, as a function of the initial velocity on *Oz direction*. Randomly positions on *Ox* and *Oy* were generated and it was obtained a number of *14003* atoms which were initially in direction of the hole ($z_0 = 2012.5nm;\ x_0$ *and* y_0 *between* $830nm$ *and* $1130nm$). The number of atoms which finally arrived in the hole ($z \le 301.875nm;$ *x and y between* $830nm$ *and* $1130nm$), as a function of the initial velocity on *Oz*, is presented in Fig.12.

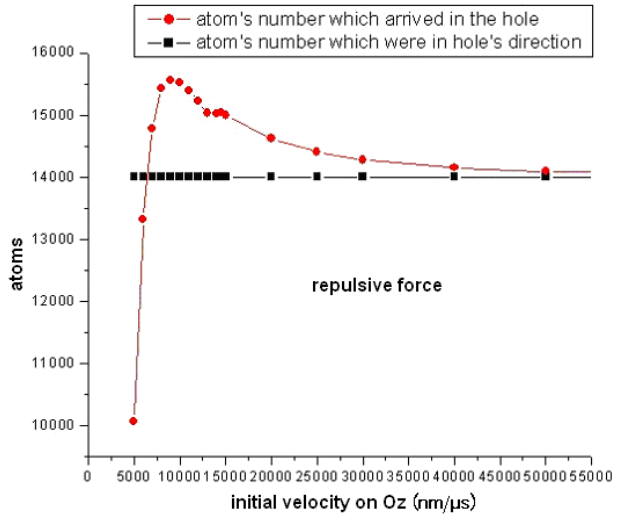

Fig. 12. The number of atoms which arrived in the hole

It can be seen from Fig. 12. that the field effect is important for initial velocity on *Oz* smaller than $15 \times 10^3\ nm/\mu s$. For initial velocities greater than $30 \times 10^3\ nm/\mu s$ the effect of the field is negligible. The time of interaction between the field and the Cs atoms is too small and the initial kinetic energy of Cs atoms is greater then the potential energy of interaction between the field and the atoms. Also, it can be seen that the number of atoms which arrive in the hole increases when the initial velocity on *Oz* decreases, till approximately $9 \times 10^3\ nm/\mu s$. The time of interaction between the field and that Cs atoms increase and so the effect of the field is greater. The fact that the more atoms arrived in the hole due to the field configuration (Fig. 6.) which presents a minimum in the hole's direction. In the "repulsive force" case the atoms will migrate there where the field is smaller.

At approximately $15 \times 10^3\ nm/\mu s$ appear the first atoms reflections due to the field configuration. From the Figs. 7-8 it can be seen that the field increases when *Oz* decreases and at one point the Cs atom will be stopped and reflected.

Between $15 \cdot 10^3\ nm/\mu s$ and $9 \cdot 10^3\ nm/\mu s$ the *collimation* effect of the electromagnetic field is greater than the effect of the *reflections* and so the number of atoms which arrive in the hole increases when the initial velocity decreases.

For initial velocities smaller than $9 \times 10^3\ nm/\mu s$ the effect of the *reflections* is greater than the *collimation* electromagnetic field effect and the number of atoms which arrive in the hole decreases when the initial velocity decreases.

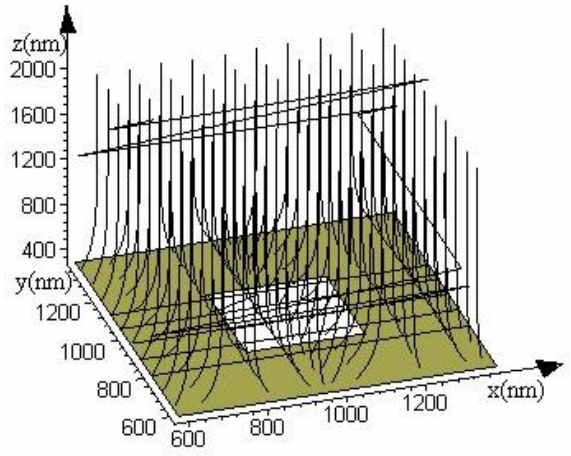

Fig. 13. 100 trajectories for v_{0z} *= -9000 nm/μs*

To see exactly what is happening with the Cs atoms in the repulsive field, trajectories were calculated and represented in Fig. 13. The initial velocity is chose to be $9 \times 10^3\ nm/\mu s$ because for this value the collimation effect of the electromagnetic field is the most important.

4. Conclusions

As it can be seen from figures 10 and 11, in the "attractive force" case, the metallic film and its scattered field can be used in order to depose Cs atoms on one side and on the other of the holes in a ($\lambda/2 = 400nm$) periodical rows photosensitive network.

In the "repulsive force" case, the metallic film and its scattered field can not be used to guide the atoms trough the holes and to depose them on a semiconductor substrate. Even if for an initial velocity of $9 \times 10^3\ nm/\mu s$ there is a collimation effect, but is very small.

References

[1] C. Cohen, Tannoudji, Atomic Motion in Laser Light, J. Dalibard, J. M.Raimond, J. Zinn-Justin, eds., Les Houches, Session LIII, (1990).
[2] C. Cohen, Tannoudji, J. Dupont-Roc, G. Grynberg, Processus d'interaction entre photons et atomes, InterEditions et Editions du CNRS, Paris,(1988).
[3] J. Weiner, Light - Matter Interaction, Volume 1 (Fundamentals and Applications), John Wiley &

Sons, Inc., Hoboken, New Jersey, (2003).
[4] G. Leveque, Etude de diffraction d'atomes froids par champs optiques confines, DEA de physique de la Matière – Université Paul Sabatier Toulouse, Juin (2000).
[5] G. Leveque, C. Meier, R. Mathevet, C. Robilliard, J. Weiner „Atomic diffraction from nanostructured optical potentials", Physical Review A, Vol. 65, (2002).
[6] F. J. Garcia - Vidal[a)], L. Martin – Moreno, H. J. Lezec, T. W. Ebbesen „Focusing light with a single subwavelength aperture flanked by surface corrugations", Applied Physics Letters, Vol. 83, No. 22, (2003).
[7] Harold J. Metcalf, Peter van der Straten „Laser Cooling and Trapping", Springer - Verlag New York, Inc., (1999).
[8] J. Moore, R. Pizer, Moment Methods in Electromagnetics, Chichester, England: Research Studies Press, (1984)
[9] M. A Morgan., Finite element and Finite Difference Methods in Electromagnetic Scattering, New York: Elsevier, (1990).
[10] S. B. Balmuș, R. Mathevet, J. Weiner, Atom manipulation with micro- and nano-structures emitted light fields, (Poster at FastNet Conference, Les Houches, France, May 2004).
[11] S. B. Balmuș, Diffraction of the high frequency electromagnetic waves on metallic and dielectric obstacles. Measurement of the dielectric permittivity by the resonant cavity method", PhD thesis, in romanian, "Al. I Cuza" University, Iasi, Romania. (Jully 2007)
[12] G. Lévêque, R. Mathevet, C. Girard, B Viaris, G. Gay, O. Alloschery, S. B. Balmuș, C. O'Dwyer, A. Balocchi, J. Weiner, Coupled resonant rings, (Poster at FastNet Conference, Les Houches, France, May 2004).

[*]Corresponding author: sorin.balmus@uaic.ro